Implementing a comprehensive hydromechanical model for sedimentary basins by coupling a 3D mechanical code to a classic basin fluid flow code with the preCICE library

J-M. GRATIEN*, D. COLOMBO*, S. DE CHAISEMARTIN*, B. VIALAY, A. PASTEAU****

* IFP Energies Nouvelles,
1 et 4 avenue Bois-Préau, 92852 Rueil-Malmaison, France
e-mail: jean-marc.gratien@ifpen.fr, daniele.colombo@ifpen.fr,
stephane.de-chaisemartin@ifpen.fr
web page: https://www.ifpenergiesnouvelles.fr
** Andra,
1 à 7 rue Jean Monnet Parc de la Croix-Blanche 92298 Châtenay-Malabry cedex, France
e-mail: bernard.vialay@andra.fr, antoine.pasteau@andra.fr
web page: https://www.andra.fr

ABSTRACT

In this paper, we present a coupling strategy for the implementation of a comprehensive hydromechanical model for sedimentary basins [1]. The preCICE framework [2] has been used to efficiently implement an iterative coupling scheme between ArcTem, a sedimentary basin fluid flow code, and Code_Aster [20], a finite element general purpose mechanical code. We discuss several issues related to different domain partitions used by the parallel codes, to the time evolutivity of the 3D meshes and to the different time stepping used by each code. We have used the preCICE framework communication system to efficiently exchange data between the codes and to interpolate fields between usually non-matching meshes. The iterative coupling scheme is managed by means of the functionalities provided by preCICE.

We validate our coupled code on a real sedimentary basin study [19]. We evaluate the flexibility of the preCICE framework to efficiently implement advanced iterative coupling algorithms. We compare the performance of our solution to a standard approach based on a centralized supervisor controlling the coupling flow and using files to exchange data between the codes.

1 Introduction

Accurate simulations are essential in the domains of energy and environment for informed decision-making, process optimization, and sustainable solutions. However, single physics models often fail to capture the complexity and intricate interactions inherent in these systems. For instance, in the field of wind energy, the design of floating wind turbines requires a combination of hydrodynamics, structural mechanics and aerodynamics. In the field of CO2 storage, radioactive waste or geothermal energy, it is necessary to simulate complex phenomena combining chemical, mechanical and porous media flow models. Multi-physics models offer a powerful solution by integrating various physical processes, providing a holistic understanding of complex systems. Two main approaches exist: the monolithic approach solves all physics equations simultaneously, offering tight coupling and global solution capability but with drawbacks of complexity, computational cost, and limited modularity. The second approach, using coupling tools, offers flexibility, modularity, and computational efficiency, although challenges lie in managing communication overhead and potential inconsistencies. Several existing coupling code frameworks, such as ASCoDT [7], CWIPI [9],EMPIRE [10], MpCCI [11], OASIS3-MCT [15], OpenPALM [14], MUSCLE [16], ONELAB [12], SALOME [13], facilitate seamless communication between solvers, promoting re-usability and compatibility. This paper focuses on the evaluation of the **preCICE** framework [2], an open-source library for coupling multi-physics simulations. This paper is organized as follow: after detailing in Section 2 the features of **preCICE**, we present in

Section 3 **A2**, a coupled hydromechanical sedimentary basin simulator, and its implementation using **preCICE** in Section 4. Validation results are presented in Section 5 and we conclude the paper in last Section 6.

2 preCICE library

The **preCICE** library is a powerful open-source tool designed for coupling multi-physics simulations, specifically targeting fluid-structure interaction problems. It provides a modular and flexible environment for seamless communication and integration between different simulation components. **preCICE** enables the coupling of various physics solvers, allowing researchers to combine specialized codes and leverage parallel computing capabilities. The library employs standardized interfaces and protocols to ensure code reusability and compatibility. It offers functionalities for data exchange, synchronization, and mapping between solvers, facilitating consistent and accurate coupling. With **preCICE**, users can easily define coupling configurations, handle different mesh types, and manage parallel simulations efficiently. The library supports both steady-state and transient simulations, enabling the modeling of complex transient phenomena. Its robust and efficient algorithms, such as the iterative fixed-point algorithm, ensure convergence and accuracy in the coupling process. **preCICE** has been widely adopted and has a growing community, providing support, documentation, and examples to facilitate its implementation in various research domains.

3 A comprehensive coupled hydromechanical sedimentary basin model

Sedimentary basin models are used to predict pore pressure and porosity distribution in the basin from its formation to present day. These models are used in oil&gas exploration, CCS (CO2 capture and storage) and geothermal energy fields. They aim at simulating and understanding the geological evolution of sedimentary basins over time. This involves integrating geological, geophysical, geomechanical and geochemical data to reconstruct the basin history and processes. For historical reasons, basin simulators usually use a simplified 1D formulation for geomechanics: sediment compaction is driven by weight only. This simplified formulation can be applied to basins in oedometric conditions. For basins where tectonics had an important role in their formation or in presence of salt layers, the strains and stresses predicted by this simplified model are erroneous. A more rigorous 3D geomechanical framework is required to capture the complex coupled hydromechanical phenomena occurring in sedimentary basins in order to assess the cap rocks integrity, the tectonic deformations, the fault reactivation risk and to correctly estimate the stress field. Such framework has been implemented in the prototype simulator **A2** by coupling **ArcTem**, a classical basin modeling code developed by IFPEN for 3D complex geometries using a simplified 1D geomechanics, and **Code_Aster** [20], an open-source advanced general-purpose mechanical 3D finite element code developed by EDF R&D.

3.1 The basin model

ArcTem, is a software package based on the open-source **Arcane** framework [6] for basin modeling with 3D complex geometries. The calculation grid is time-dependent. Its kinematic is imposed by the geological structural restoration carried out before the flow simulation: this 4D grid is built after restoration to meet the requirements of forward simulation. Sediment deposition and tectonic episodes, corresponding to geological events, are discretized into a sequence of static grids. Physical quantities are transferred between grids at transition points. These static grids are gathered into a time evolutive 3D mesh that constitutes the basin 4D grid. The evolutive 3D mesh enables to model complex geometries with faults. An example is shown in Figure 1 where a simple basin representation is visible showing the complexity of the 3D geometry and faults configuration generating non conformity of the meshes.

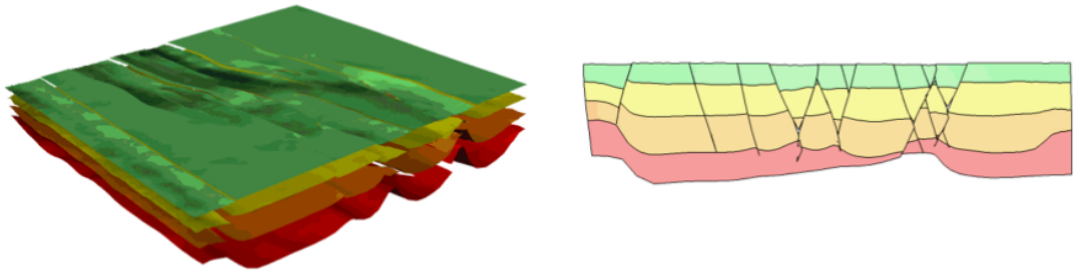

Figure 1: Example of sedimentary basin model with faults - On the left: 3D representation of horizons, the surfaces between two sedimentary layers - On the right: a cross section of the model clearly showing the faults configuration

In basin modeling several physical processes are simulated. The equations used to represent these processes depend on the complexity and scope of the simulation. However some fundamental equations are always used. As presented in details in [5], fluid flow coupled with compaction is governed by the following set of equations:

- mass conservation of solid:

$$\frac{\partial}{\partial t}(\rho_s(1-\Phi)) + \nabla \cdot (\rho_s(1-\Phi)\mathbf{v_s}) = \rho_s q_s \tag{1}$$

  where q_s is the sediment deposition rate, Φ is the sediment porosity, $\mathbf{v_s}$ the solid velocity and ρ_s the solid density;

- mass conservation of fluid:

$$\frac{\partial}{\partial t}(\rho_w \Phi) + \nabla \cdot (\rho_w \Phi \mathbf{v_w}) = \rho_w q_w \tag{2}$$

  where q_w is the water flux associated to sediment deposition, which is expressed as a function of the sediment porosity: $q_w = q_s \Phi_0/(1-\Phi_0)$, ρ_w is the water density and $\mathbf{v_w}$ is the water velocity;

- Darcy's law:

$$\mathbf{u}_w = \Phi(\mathbf{v_w} - \mathbf{v_s}) = -\frac{K_m}{\mu_w}(\nabla P - \rho_w \mathbf{g}) \tag{3}$$

  where $\mathbf{u}_w$ is the water flux, μ_w is the water viscosity, K_m is the sediment permeability, P the fluid pore pressure and $\mathbf{g}$ is the gravity;

- sedimentary vertical load:

$$-\frac{\partial}{\partial z}\sigma_l = (\rho_s(1-\Phi) + \rho_w \Phi)g \tag{4}$$

  where σ_l is the vertical stress given by the weight of sediments;

- compaction law:

$$\Phi = F_\Phi(\sigma) \tag{5}$$

  where porosity Φ is expressed as a function of the effective stress $\sigma = \sigma_l - P$. This function is lithology dependent and it accounts for sediment compaction due to sediments weight only.

These equations are completed with other sediment constitutive laws (permeability as a function of porosity, fluid density and viscosity as a function of pressure) and appropriate boundary conditions:

- assuming an offshore basin, the top boundary is subjected to the sea water pressure:

$$\sigma_l(top) = P_{top} \tag{6}$$

- on the bottom boundary, no fluid flow is assumed:

$$\mathbf{u_w} \cdot \mathbf{n} = 0 \tag{7}$$

In order to highlight the coupling between these equations and the link between them and the geometry, we reformulate the equations using the overpressure oP and the lithostatic potential $\tilde{\sigma}$ defined as $\tilde{\sigma_l} - P_h$ and $oP = P - P_h$, respectively. The hydrostatic pressure P_h satisfies the following equation:

$$-\frac{\partial}{\partial z} P_h = \rho_w g \tag{8}$$

and the boundary condition $P_h = P_{top}$ on the top boundary.

3.2 The geomechanical model

Code_Aster is coupled to **ArcTem** in order to implement a full 3D geomechanical framework going beyond the simplified 1D geomechanics used in **ArcTem**. **Code_Aster** is an open-source general-purpose mechanical finite element code. The availability of the source code has permitted to adapt the code for the hydromechanical coupling with **ArcTem**.

Even if THM capabilities for porous media are available in **Code_Aster**, they have not been used in the coupling. Indeed, fluid flow simulation capabilities of **ArcTem** are much more advanced than the ones available in **Code_Aster** THM models.

A standard non-porous mechanical simulation is carried out in **Code_Aster**. Fluid is introduced in the mechanical simulation as an external load. The equilibrium equation, based on the total stress, is rewritten in terms of the complete 3D effective stress tensor:

$$\nabla \cdot \boldsymbol{\sigma} = \nabla \cdot P\mathbf{I} - \mathbf{b} \tag{9}$$

where $\mathbf{I}$ is the second order identity tensor and $\mathbf{b}$ is the vector of body forces. In the definition of the effective stress, Biot's coefficient has been taken equal to one.

Equation (9) shows that fluid pore pressure P is introduced in the mechanical equilibrium equation as an external load coming from the **ArcTem** fluid flow simulation. Since sediments compaction induces strong changes in sediments volume, a finite strain formulation is used. An updated lagrangian scheme [17] is adopted to solve the equations by a sequence of infinitesimal strain problems. Therefore the strain tensor is calculated as:

$$\boldsymbol{\epsilon} = \frac{1}{2}(\nabla \mathbf{u} + (\nabla \mathbf{u})^T) \tag{10}$$

where $\mathbf{u}$ is the displacement vector. Sediment porosity is calculated from the strain tensor by calculating the infinitesimal volume change: change in porosity is assumed to be equal to the infinitesimal volume change. This is a consequence of the Biot's coefficient value used in the

derivation of equation (9), which means that an incompressible skeleton is assumed for the bulk material and volume changes are accommodated by porosity changes.

An elastoplastic constitutive equation derived from the compaction law (5) is used for the sediments [1]. This equation is a modified version of the Cam-Clay model accounting for vertical and lateral compaction of the sediments by extending to the 3D case the Schneider 1D compaction law [18] used in **ArcTem**.

Fracture of sediments is assumed to occur when the stress state crosses the critical state line of the Cam-Clay plastic yield surface, entering in the dilation part. Sediment permeability is increased to account for sediment fracture by a coefficient multiplying the permeability used by **ArcTem**. The value of this coefficient increases with the cumulated plastic strain.

3.3 The hydromechanical coupling scheme

Coupling the hydrogeological and geomechanical models enables the investigation of interactions between fluid flow, pore pressure changes and mechanical deformation, providing insights into the subsurface system behavior. However, coupling the two codes involves addressing several challenges. The evolutionary nature of the meshes and non-linearity of the models require implementing an iterative coupling scheme to obtain correct results. Convergence of the iterative coupling scheme is checked against the porosity values calculated in the two codes independently.

The basin simulation consists of a sequence of geological events. The coupling scheme operates at the event level (Figure 2). Sequential coupling starts with an **ArcTem** simulation using geometries coming from the preliminary geological restoration phase. This simulation evaluates pore pressure and porosity evolution for the event. The pore pressure values are then transferred to **Code_Aster**, which simulates the same event from the beginning (Figure 3). The porosity values obtained by **Code_Aster** are compared cell by cell with those calculated by **ArcTem**. If the difference is below a specified tolerance for most cells, convergence is achieved, and coupling proceeds to the next event. Otherwise, a new iteration is performed: **Code_Aster** calculates a correction ($\Delta\sigma$) sent to **ArcTem** before replaying the event (Figure 4). This correction is evaluated by means of the 1D compaction law (5) used by **ArcTem**:

$$\Delta\sigma = F_{\Phi}^{-1}(\Phi_{\mathbf{ArcTem}}) - F_{\Phi}^{-1}(\Phi_{\mathbf{Code\_Aster}}) \tag{11}$$

Once convergence is reached, **Code_Aster** evaluates the fracturing criterion and calculates the permeability multiplicative factor for cells where the criterion is verified. The multiplicative factor is sent to **ArcTem** for the subsequent event (Figure 4).

The coupling scheme is sequential, with the basin code running first and the mechanical code waiting for results. It is an implicit scheme utilizing an iterative fixed-point algorithm to ensure convergence of computed porosity within a specified tolerance.

4 Details on the coupling implementation with preCICE

The coupled hydromechanical model of **A2** presented in the previous section 3 has been implemented with **preCICE**, version 2.3. Figure 5 illustrates the architecture of our implementation. We have developed for the two coupled codes a **preCICE** adaptor. The **Code_Aster** adaptor has been developed using the python **preCICE** API while the **ArcTem** one has been developed in C++. This adaptor provides helpers to define the coupling mesh zones and the coupling fields to exchange, to parameterize interpolation and numerical coupling algorithms and to access the advanced functions available in **preCICE**. As the dynamic adaptive mesh feature was not available in the used **preCICE** version, we have developed an original strategy to handle dynamic

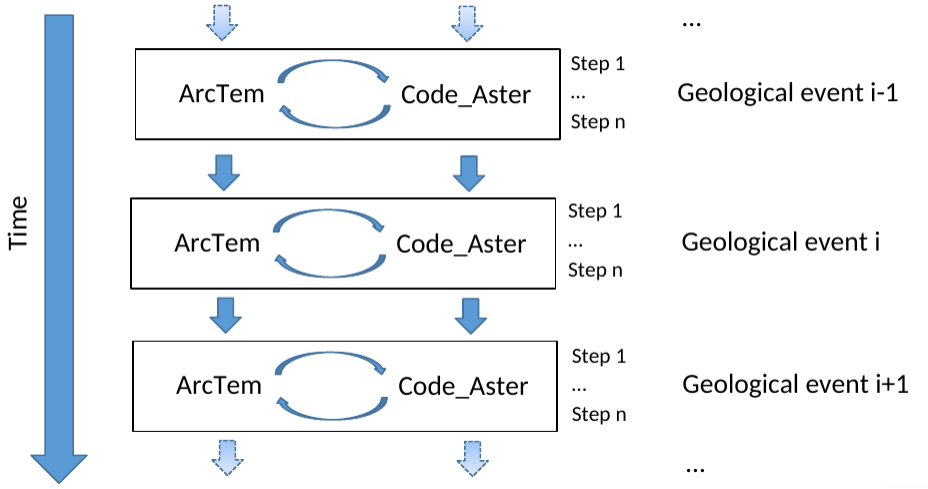

Figure 2: Coupling scheme used for the simulation

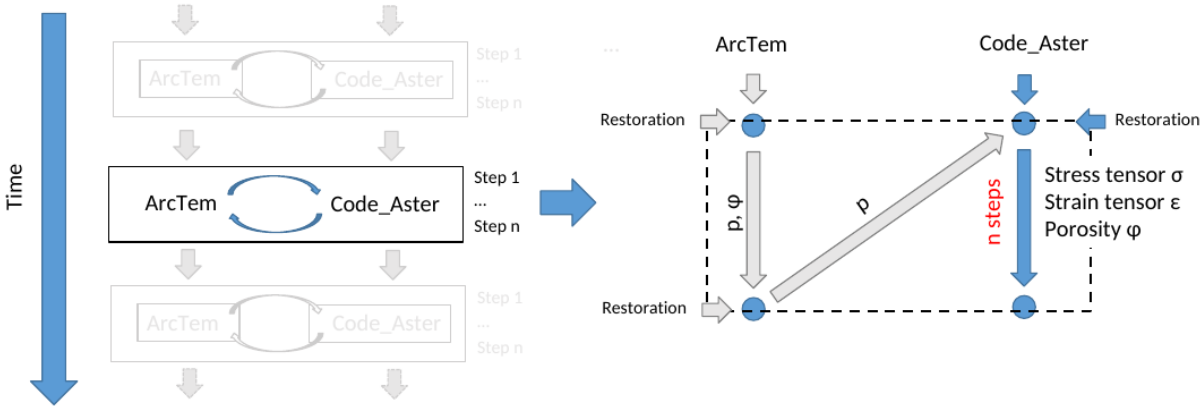

Figure 3: Details of the sequential iterative scheme used for each geological event

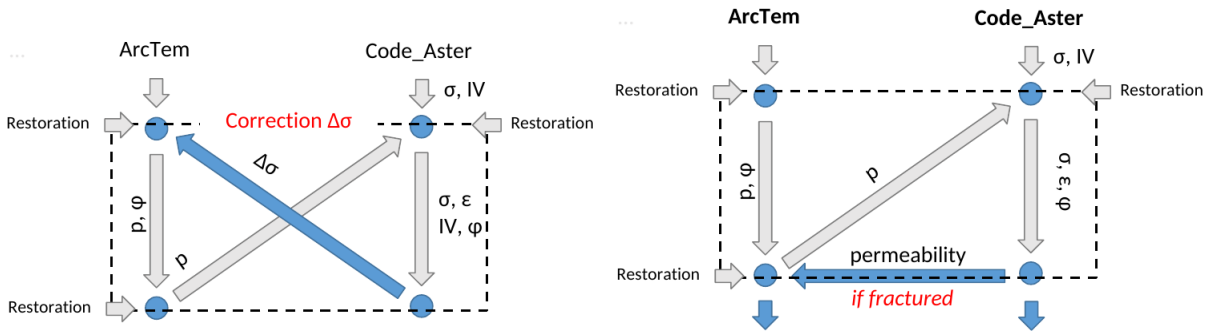

Figure 4: Data exchanged at the end of each geological event. On the left: correction $\Delta\sigma$ calculated in the case of non-convergence of the iterative scheme. On the right: calculation of the new permeability when fracture occurs.

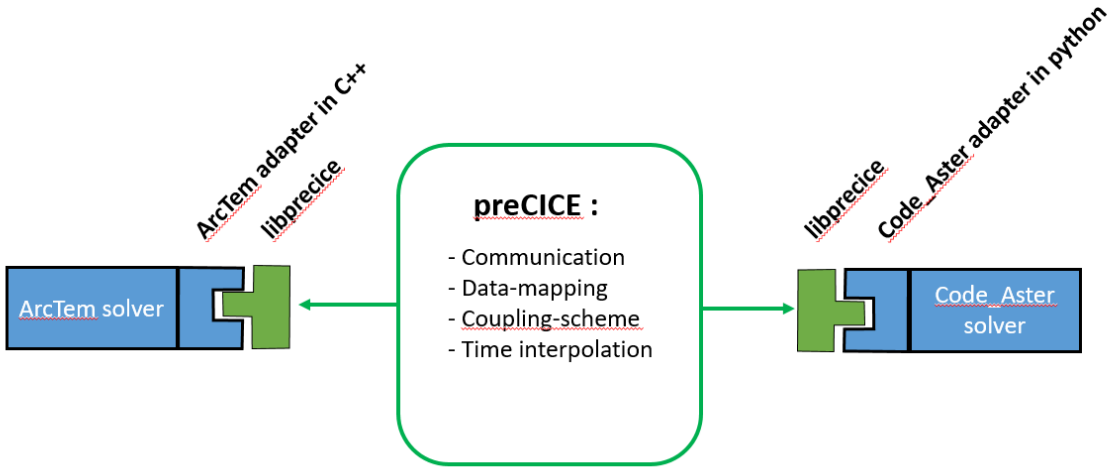

Figure 5: **A2** architecture using preCICE

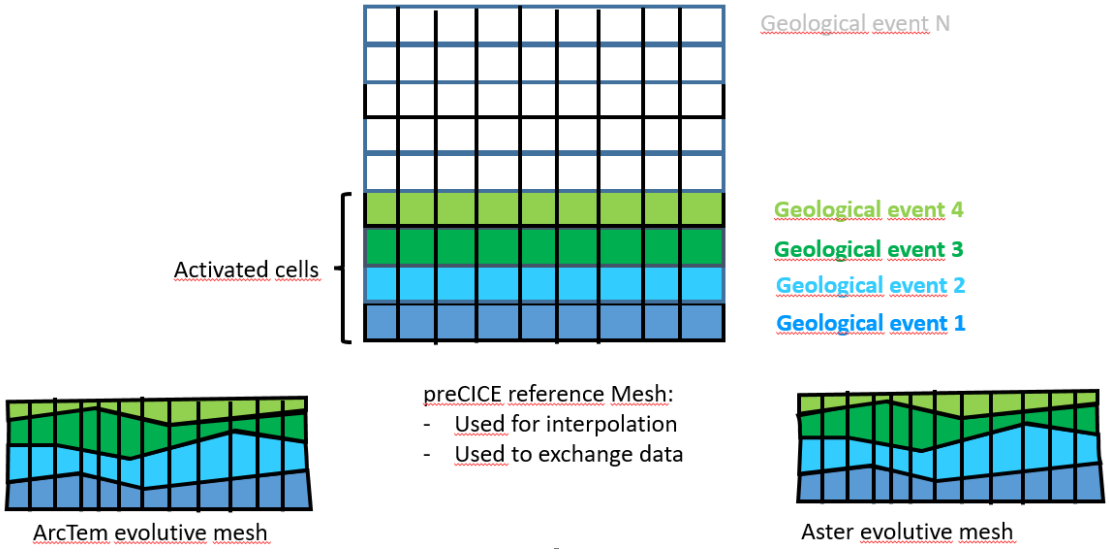

Figure 6: **ArcTem**, **Code_Aster** evolving meshes and **preCICE** reference mesh

evolving meshes. We have introduced an intermediate **preCICE** reference mesh used at the library initialization. All mapping, partitioning and communication structures are initialized statically once at the begin of the simulation. This reference mesh is related to the state of the last geological event and contains all the grid cells appearing in the model through the whole simulation. The mapping between **ArcTem** and the **Code_Aster** evolving meshes and this reference mesh is realized by grid cell unique label ids. To reduce the amount of data exchanged at each coupling step, we have introduced in **preCICE** new functionalities to manage mesh filters to define the concept of activated cells. Thus during a coupling step, the mapping is only realized on activated cells and only the data related to these cells are exchanged. At the first step of new geological event, when a new sedimentary layer is deposited, we update mesh filters by activating in the reference mesh the cells related to the new deposited sedimentary layer. Figure 6 illustrates **ArcTem** and **Code_Aster** evolving mesh after 4 geological events, and the **preCICE** reference mesh containing all the grid cells related to a number N of events.

The convergence criterion of the iterative coupling algorithm used in our coupling scheme is very specific to our model and was not available among the convergence criteria provided by **preCICE**. We have therefore modified the **preCICE** API to enable **Code_Aster** to send

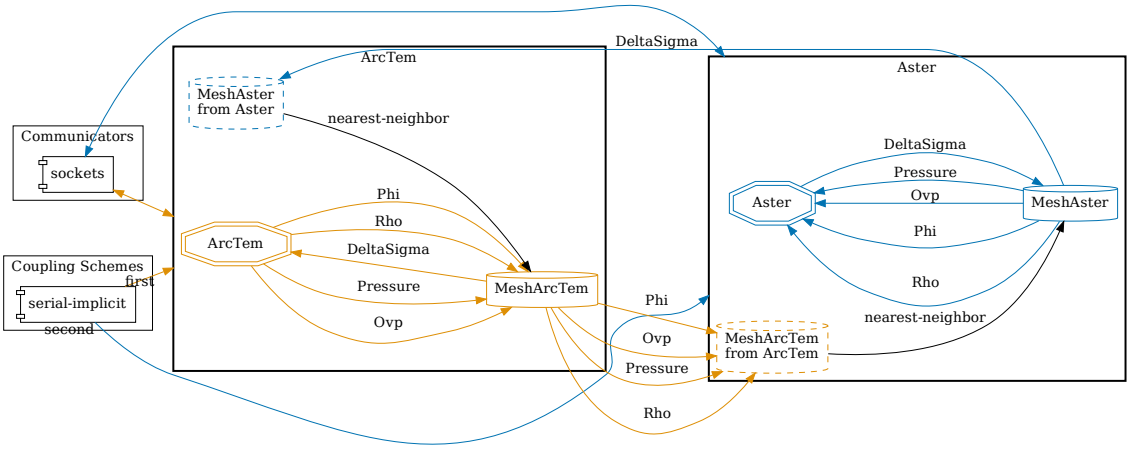

Figure 7: Sequential iterative scheme used during each geological event

to **ArcTem** , by means of **preCICE** communication capabilities, the result of a convergence criterion evaluated by itself, deactivating the convergence criterion check done by **preCICE**.

Figure 7 represents the diagram of the coupling scheme: a serial implicit coupling scheme is used with an iterative fixed point algorithm controlled by a convergence criterion evaluated on the exchanged porosity field. The exchanged fields (P, Φ, $\Delta\sigma$ and oP) are represented by the links with the field name between each solver meshes.

5 Results

We validated the **A2** implementation with **preCICE** using the Neuquén basin real case described in [19]. The model dimensions span approximately 200 km in the horizontal plane and 8 km in depth. It consists of 20 geological layers, and the simulation incorporates a total of 39 events, including layer deposition, uplift, erosion, and tectonic phases. The **preCICE A2** simulation was completed up to event 19, representing a period of stability in the Neuquén basin before the final uplift and tectonic phase. The mesh at event 19 is composed by 102,000 cells, partitioned into 72 partitions for **Code_Aster** and 4 partitions for **ArcTem** (Figure 8).

We compare in Figure 9 the performance obtained with our implementation to the one obtained with the legacy **A2** implementation based on a centralized supervisor controlling the coupling flow. This supervisor uses files on disk to exchange data between the codes and restart mechanisms of the two simulation codes to replay the simulation of the geological events during the iterative coupling algorithm. In spite of the small model size used in the test, significant reduction in computation time is achieved by the **preCICE A2** version compared to the legacy version. The **preCICE** communication mechanism reveals superior performances compared to the data exchange mechanism based on files on disk, as clearly shown by the comparison of data exchange times between **ArcTem** and **Code_Aster** during the simulation.

From a development perspective, the utilization of the **preCICE** API significantly reduced the amount of technical code required for the coupling implementation. The need for a centralized supervisor and the associated services and MPI communications for generating and reloading restart dump files in both **ArcTem** and **Code_Aster** were eliminated. The versatility and user-friendliness of the **preCICE** API enabled the development of a minimal number of C++ and Python code lines, integrated into **ArcTem** and **Code_Aster** respectively.

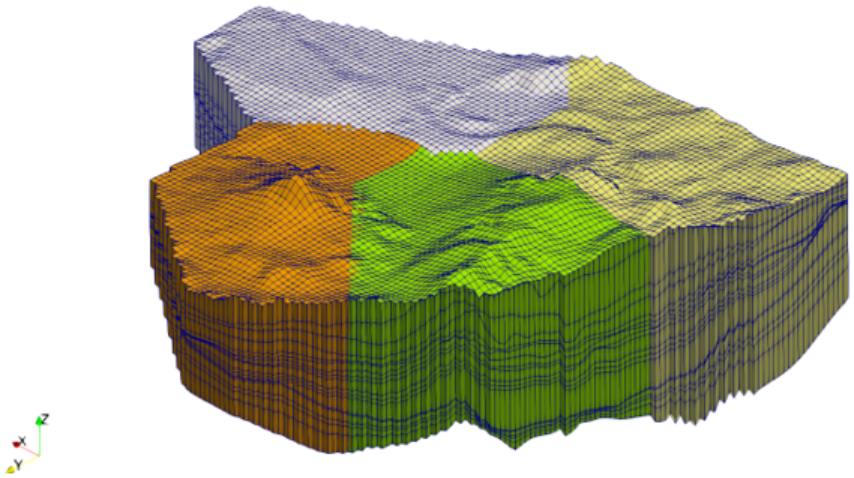

Figure 8: Mesh used for the Neuquén model at geological event 19 - For sake of clarity, only 4 mesh partitions are shown whereas the simulation has been done on 72 partitions

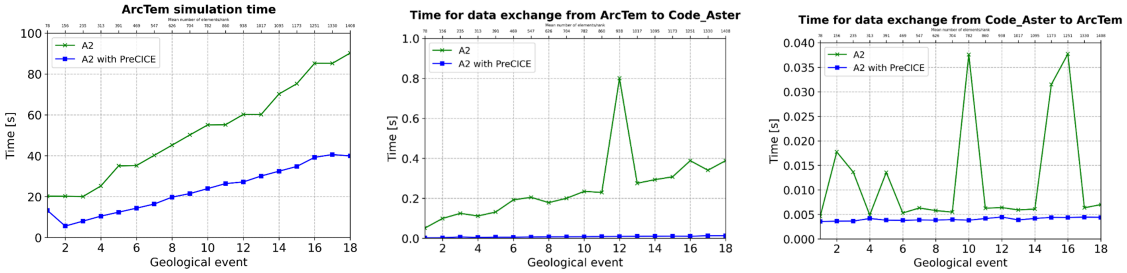

Figure 9: Comparison of performances of **legacy A2** and **preCICE A2** versions

6 Conclusion and perspectives

We have presented a comprehensive hydromechanical model for sedimentary basins based on the coupling of **ArcTem**, a sedimentary basin fluid flow code, and **Code_Aster**, a finite element general-purpose mechanical code. The coupling strategy used in this study relies on the **preCICE** framework, which facilitated the implementation of an iterative coupling scheme. By leveraging the features of **preCICE**, we successfully addressed various challenges associated with the management of time-evolving 3D meshes. Additionally, the flexibility of the framework allowed for the development of new functionalities to handle 4D evolving meshes and to incorporate a specific convergence criterion for the iterative coupling algorithm. The validity of our coupled code was demonstrated through its application to a real sedimentary basin study. The performance results obtained show significant reduction in computation time when using the **preCICE** library compared to a standard approach relying on a centralized supervisor and file-based data exchange between the codes. In future works, we would like to validate our approach by incorporating erosion, which involves the disappearance of grid cells during simulation. Further testing is required to develop specific meshes tailored to each coupled model, enhancing the accuracy and applicability of our framework.

REFERENCES

[1] Bruch A., Colombo D., Frey J., et al. Coupling 3D geomechanics to classical sedimentary basin modeling: From gravitational compaction to tectonics. Geomechanics for Energy and the Environment, 2021, vol. 28, p. 100259.

[2] CHOURDAKIS, Gerasimos, DAVIS, Kyle, RODENBERG, Benjamin, et al. preCICE v2: A sustainable and user-friendly coupling library. arXiv preprint arXiv:2109.14470, 2021.

[3] Toutin Thierry. ASTER DEMs for geomatic and geoscientific applications: a review. International Journal of Remote Sensing, 2008, vol. 29, no 7, p. 1855-1875.

[4] Cacas-Stentz M.C., Arbeaumon A., Faille I., et al. New Tools and Workflow to Model Petroleum Systems in Structurally Complex Basins. In : Tyumen 2015-Deep Subsoil and Science Horizons. European Association of Geoscientists and Engineers, 2015. p. 1-5.

[5] Faille, I., Thibaut, M., Cacas, M. C., Havé, P., Willien, F., Wolf, S., ... & Pegaz-Fiornet, S. (2014). Modeling fluid flow in faulted basins. Oil & Gas Science and Technology–Revue d'IFP Energies nouvelles, 69(4), 529-553.

[6] Grospellier, Gilles and Lelandais, Benoit, The Arcane Development Framework, Proceedings of the 8th Workshop on Parallel/High-Performance Object-Oriented Scientific Computing, 2009.

[7] A. Atanasov, H.J. Bungartz, and T. Weinzierl. A Toolkit for the Code Development in Advanced Computing. Report, Technische Universität München (TUM), Munich,Germany, 2013.

[8] `http://adventure.sys.t.u-tokyo.ac.jp/`

[9] `http://sites.onera.fr/cwipi/`

[10] http://empire.st.bv.tum.de, T. Wang, S. Sicklinger, R. Wüchner, and K.-U. Bletzinger. "Concept and Realization of Coupling Software EMPIRE in Multiphysics Co-Simulation". Proceedings of the V International Conference on Computational Methods in Marine Engineering (Marine) 2013, pp. 289–298, Hamburg, Germany, 2013.

[11] http://congress.cimne.com/marine2013/frontal/ProgSesion.asp?id=44, http://www.mpcci.de/, MpCCI 4.4.1-1 Documentation. Documentation, Fraunhofer Institute for Algorithms and Scientific Computing (SCAI), Sankt Augustin, Germany, 2015.

[12] C. Geuzaine, F. Henrotte, J.-F. Remacle, and R.V. Sabariego. "ONELAB: Bringing Open-Source Simulation Tools to Industry Design and Education". Proceedings of the Conference on the Computation of Electromagnetic Fields (COMPUMAG) 2015, pp. 1–2, Montréal, Canada, 2015. http://lirias.kuleuven.be/bitstream/123456789/479419/1/onelab_abstract_cmag2015.pdf

[13] http://www.salome-platform.org/

[14] A. Thévenin. OASIS3-MCT & Open-PALM: 2 open source codes couplers. Presentation, Centre Européen de Recherche et de Formation Avancée en Calcul Scientifique (CERFACS), Toulouse, France, 2012.

[15] http://verc.enes.org/oasis/

[16] http://www.qoscosgrid.org/trac/muscle, J. Borgdorff, M. Mamonski, B. Bosak, K. Kurowski, M. Ben Belgacem, B. Chopard, D. Groen, P.V. Coveney, and A.G. Hoekstra. "Distributed Multiscale Computing with MUSCLE 2, the Multiscale Coupling Library and Environment". Journal of Computational Science, vol. 5, no. 5, pp. 719–731, Elsevier, 2014.

[17] K.J.Bathe, Finite Element Procedure, Precentice-Hall, 1996

[18] Schneider F, Wolf S, Faille I, Pot D. "A 3D basin model for hydrocarbon potential evaluation: Application to Congo offshore", Oil Gas Sci Technol - Rev IFP. 2000;55:3–13.

[19] Berthelon J, Bruch A, Colombo D, Frey J, Traby R, Bouziat A, Cacas-Stentw M.C., Cornu T., "Impact of tectonic shortening on fluid overpressure in petroleum system modelling: insights from the Neuquén basin, Argentina", Marine and Petroleum Geology, 127 (2021) 104933

[20] http://www.code-aster.org